Udenfriend, S., Stein, S., Bohlen, P., Dairman, W., Leimgruber, W., & Weigele, M. (1972) *Science (Washington, D.C.) 178*, 871–872.
Weber, K., & Osborn, M. (1975) in *The Proteins* (Neurath, H., Hill, R. L., & Boeder, C.-L., Eds.) 3rd ed., Vol. I, pp 179–223, Academic Press, New York.
Woods, K. R., & Wang, K. T. (1967) *Biochim. Biophys. Acta 133*, 369–370.
Wun, K. L., Gih, A., & Sutherland, J. C. (1977) *Biochemistry 16*, 921–924.

Elementary Steps in the Reaction Mechanism of the Pyruvate Dehydrogenase Multienzyme Complex from *Escherichia coli*: Kinetics of Acetylation and Deacetylation†

Steven K. Akiyama‡ and Gordon G. Hammes*

ABSTRACT: The kinetics of the acetylation of the pyruvate dehydrogenase complex from *Escherichia coli* by [3-^{14}C]pyruvate and of the deacetylation of the complex by coenzyme A have been studied by using rapid mixing–quench techniques. The time course for acetylation in 4 mM thiamin pyrophosphate, 2 mM $MgSO_4$, and 0.02 M potassium phosphate (pH 7.0) at 4 °C can be analyzed in terms of two kinetic processes. At long times 10 nmol of acetyl groups is incorporated per mg of enzyme complex (48 sites per complex of molecular weight 4.8×10^6). The slower process is much too slow to be of catalytic significance. The rate constant for the faster process is not dependent on enzyme concentration and reaches a limiting value of 40–65 s^{-1} at high pyruvate concentrations; the exact value is dependent on the detailed acetylation mechanism assumed. The minimum molar turnover number of the enzyme complex is 420 s^{-1} (17.5 s^{-1} per pyruvate decarboxylase). The acetylated lipoic acids are deacetylated by coenzyme A at a rate much faster than that of acetylation. Complete deacetylation is obtained only if the deacetylation is carried out within seconds of the acetylation, apparently because dead-end intramolecular transfers of acetyl groups from the lipoic acids to other functional groups on the enzyme not essential for catalytic activity can occur. The results obtained suggest only about half of the acetylation reactions are on the main catalytic pathway.

The pyruvate dehydrogenase multienzyme complex of *Escherichia coli* consists of three different enzymes (Koike et al., 1963; Willms et al., 1967) with a polypeptide-chain stoichiometry of 24 pyruvate decarboxylases (E_1),[1] 24 dihydrolipoyl transacetylases (E_2), and 12 dihydrolipoyl dehydrogenases (E_3) and an overall molecular weight of 4.8×10^6 (Reed, 1974; Angelides et al., 1979). These enzymes catalyze the decarboxylation of pyruvic acid and the acetylation of coenzyme A by the following sequence of reactions (Koike et al., 1960):

$$\text{pyruvate} + E_1[\text{TPP}] \rightarrow CO_2 + E_1[\text{hydroxyethyl-TPP}] \quad (1)$$

$$E_1[\text{hydroxyethyl-TPP}] + E_2[\text{Lip-(S)}_2] \rightleftharpoons E_1[\text{TPP}] + E_2[\text{HS-Lip-S-acetyl}] \quad (2)$$

$$E_2[\text{HS-Lip-S-acetyl}] + \text{coenzyme A} \rightleftharpoons E_2[\text{Lip-(SH)}_2] + \text{acetyl coenzyme A} \quad (3)$$

$$E_2[\text{Lip-(SH)}_2] + E_3[\text{FAD}] \rightleftharpoons E_2[\text{Lip-(S)}_2] + E_3[\text{FAD(red.)}] \quad (4)$$

$$E_3[\text{FAD(red.)}] + NAD^+ \rightleftharpoons E_3[\text{FAD}] + \text{NADH} + H^+ \quad (5)$$

where TPP, Lip-$(S)_2$, and Lip-$(SH)_2$ are thiamin pyrophosphate and oxidized and reduced lipoic acid, respectively. The brackets indicate cofactors and intermediates which are tightly or covalently bound to the enzyme.

The mechanism of the overall reaction involves the interaction of a lipoic acid with the catalytic sites of all three enzymes. Resonance energy transfer measurements suggest that a single lipoic acid cannot span the distances between the catalytic sites (Moe et al., 1974; Shepherd & Hammes, 1976, 1977) and that lipoic acid residues are in close proximity to each other (Angelides & Hammes, 1979). Studies of the overall activity of chemically modified enzyme complexes indicate that at least two lipoic acids are required per catalytic cycle and that only about seven active lipoamide dehydrogenases are required for a completely active complex (Angelides & Hammes, 1978). Thus, the mechanism for the overall reaction very likely involves the transfer of acetyl groups and oxidation–reduction between lipoic acids (Brown & Perham, 1976; Bates et al., 1977; Collins & Reed, 1977; Angelides & Hammes, 1978).

For further elucidation of the reaction mechanism, a study of the individual steps in the reaction mechanism utilizing fast reaction techniques has been initiated. In this work the acetylation and deacetylation of the complex (eq 1–3) have been studied by using quenched stopped-flow techniques. The acetylation of the lipoic acids occurs by two pathways, with only one of the pathways being sufficiently rapid to be involved in the overall catalysis. The rate of acetylation via the faster pathway reaches a limiting value at high pyruvate concentrations, 0.02 M potassium phosphate (pH 7.0), and 4 °C, which is greater than the minimum turnover number of the complex under identical conditions. In the catalytic cycle, the rate of deacetylation of the lipoic acids by coenzyme A is much faster than the rate of acetylation; furthermore, pathways exist

† From the Department of Chemistry, Cornell University, Ithaca, New York 14853. *Received November 30, 1979.* This work was supported by grants from the National Institutes of Health (GM 13292) and the National Science Foundation (PCM77-11392).

‡ National Institutes of Health Predoctoral Trainee (GM 00834 and GM 07273).

[1] Abbreviations used: E_1, pyruvate decarboxylase; E_2, dihydrolipoyl transacetylase; E_3, dihydrolipoyl dehydrogenase; NAD^+, nicotinamide adenine dinucleotide; NADH, reduced nicotinamide adenine dinucleotide.

0006-2960/80/0419-4208$01.00/0

for the dead-end intramolecular transfer of acetyl groups from lipoic acids to other reactive groups on the enzyme complex.

Experimental Section

Materials. The [3-^{14}C]pyruvate (15–25 Ci/mol) was obtained as the sodium salt from Amersham and New England Nuclear. It was dissolved in 0.02 M potassium phosphate (pH 7.0) to yield a stock solution of ~250 μCi/mL. The pyruvate concentration of this stock solution was determined by the lactate dehydrogenase assay (Meister, 1950). The stock solution was stored at −10 °C for no more than 5 days. In some cases the pyruvate was purified by preparative paper chromatography in ethanol–methanol–water (9:9:2) (Neish, 1957); identical results were obtained with the purified and commercial materials. The unlabeled pyruvate, thiamin pyrophosphate, coenzyme A, dithiothreitol, NAD (grade V), and serum albumin (bovine) were purchased from Sigma Chemical Co., and enzyme-grade ammonium sulfate was from Schwarz/Mann. All other chemicals were the best available commerical grades, and all solutions were prepared with deionized, distilled water.

Pyruvate Dehydrogenase Complex. The pyruvate dehydrogenase complex was prepared from frozen *E. coli* cell paste (Strain B, late-log harvest, Miles Laboratories) by the method of Reed & Willms (1966). An ammonium sulfate precipitation (22.5 g of ammonium sulfate/100 mL) was used to separate the pyruvate dehydrogenase complex from the α-ketoglutarate complex. If the specific activity was unusually low, further purification was effected by an isoelectric precipitation at pH 4.9 (Reed & Willms, 1966). The enzyme was dialyzed against 0.1 M potassium phosphate, pH 8.25, and 3 mM ethylenediaminetetraacetic acid to remove the bound thiamin pyrophosphate (Shepherd & Hammes, 1976), followed by dialysis against 0.02 M potassium phosphate (pH 7.0) before use. The specific activity of the pyruvate dehydrogenase complex as measured by the reduction of NAD^+ in 5 mM pyruvate, 0.5 mM thiamin pyrophosphate, 2 mM $MgCl_2$, 3 mM NAD^+, 0.2 mM coenzyme A, 2 mM dithiothreitol, and 0.1 M potassium phosphate (pH 8.0) at 30 °C was between 33 and 38 μmol of NADH formed per min per mg of protein. The protein concentration was determined by the method of Lowry et al. (1951) by using bovine serum albumin as a standard with a correction factor of 0.93 and a molecular weight of 4.76×10^6 (Angelides et al., 1979). The purity of the enzyme also was checked by polyacrylamide gel electrophoresis (Shepherd & Hammes, 1977).

Steady-State Kinetics. The steady-state kinetic experiments were done in 0.02 M potassium phosphate (pH 7.0) by using a Cary 118 spectrophotometer and monitoring the formation of NADH at 340 nm. The cell compartment was thermostated at 4 °C and was purged with argon.

Acetylation Kinetics. The time course for the acetylation of the pyruvate dehydrogenase complex by [3-^{14}C]pyruvate was followed by use of a combined quenched flow (Lymn & Taylor, 1970) and pulsed quenched flow apparatus (Fersht & Jakes, 1975) which is described in detail elsewhere (Akiyama, 1980). Concentrated enzyme (~20–25 mg/mL) was transferred to deaerated 0.02 M potassium phosphate (pH 7.0), 4 mM thiamin pyrophosphate, and 2 mM $MgSO_4$. The [3-^{14}C]pyruvate was diluted with unlabeled pyruvate and dissolved in the same buffer. The final specific activity of the [3-^{14}C]pyruvate ranged from 4×10^6 to 3×10^7 cpm/μmol of pyruvate. After incubation of the enzyme with thiamin pyrophosphate for at least 10 min on ice, the enzyme and pyruvate solutions were loaded into the apparatus and equilibrated at 4 °C. For each point on the time course, 0.3 mL each of the enzyme and pyruvate solutions was mixed. The reaction was quenched by adding concentrated perchloric acid to a final concentration of 10%, which precipitated the acetylated enzyme. The precipitate was stored on ice for between 30 and 120 min and then collected on a Whatman GF/C filter by using a stainless steel filter apparatus. The filter was washed with five 4-mL aliquots of ice-cold 10% perchloric acid, followed by two 4-mL washes with ice-cold 95% ethanol. The filter was dried on the filter apparatus with the suction on for 5 min. The filter was then placed in a scintillation vial with 10 mL of Aqueous Counting Scintillant (Amersham) for at least 12 h before counting in a Beckman LS-255 liquid scintillation counter. A background radioactivity correction was determined by reacting the enzyme complex with [3-^{14}C]pyruvate in the absence of thiamin pyrophosphate and Mg^{2+}, followed by quenching and washing as described above. An average value of 200 cpm was obtained for several samples over a range of incubation times and was subtracted from each point in the time course. The radioactivity of the filters during an acetylation experiment ranged from about 1000 to 25 000 cpm. When trichloroacetic acid (10% final concentration) was used to precipitate the labeled enzyme and wash the filter, erratic results were obtained and ~45–60% of the label was lost from the protein.

Deacetylation Kinetics. The deacetylation reaction was studied in 0.02 M potassium phosphate (pH 7.0) at 4 °C either by mixing the enzyme incubated in 4 mM thiamin pyrophosphate and 4 mM $MgSO_4$ with 0.05 or 1.4 mM pyruvate, 0.2 mM coenzyme A, and 2 mM dithiothreitol or by acetylating the enzyme complex by addition of 0.64 mM labeled pyruvate to the incubation mixture and mixing with 0.2 or 0.3 mM coenzyme A and 2 mM dithiotheitol. The mixing and quenchings were done manually or in the quenched-flow apparatus, depending upon the time span of the experiment. Deacetylation of the prelabeled enzyme was also carried out in the presence of 15 mM NAD^+.

Data Analysis. The steady-state and acetylation kinetic data were analyzed with a nonlinear least-squares program on a PDP-11 computer.

Results

The turnover number of the enzyme complex and the dependence of the steady-state velocity, v, on the concentrations of NAD^+ and pyruvate were determined at 4 °C in 0.02 M potassium phosphate (pH 7.0), 4 mM thiamin pyrophosphate, 2 mM $MgSO_4$, 0.5 mM dithiothreitol, and 0.2 mM coenzyme A. The range of NAD^+ concentration was 0.074–3.28 mM, and that of pyruvate was 0.015–7.23 mM. When the pyruvate concentration was varied, the NAD^+ concentration was 3 mM, and, when the NAD^+ concentration was varied, the pyruvate concentration was 5 mM. The enzyme concentration was 0.36–0.46 nM. The results obtained are summarized in Figure 1 as plots of the initial velocity divided by the total enzyme concentration vs. the concentration of NAD^+ and pyruvate, respectively. The data were fit to the simple Michaelis–Menten equation

$$v/[E_0] = k_{cat}/(1 + K_m/[S]) \qquad (6)$$

were $[E_0]$ is the total enzyme concentration, k_{cat} is the turnover number, and K_m is the apparent Michaelis constant of the substrate, S. Least-squares analysis gave $k_{cat} = 408\ s^{-1}$ and $K_m = 0.176$ mM for NAD^+ and $k_{cat} = 436\ s^{-1}$ and $K_m = 0.410$ mM for pyruvate. The turnover number was independent of the enzyme concentration over a range of 0.049–16 nM. When the NAD^+ concentration is greater than 3.2 mM, inhibition of the initial velocity is observed. This inhibition may be

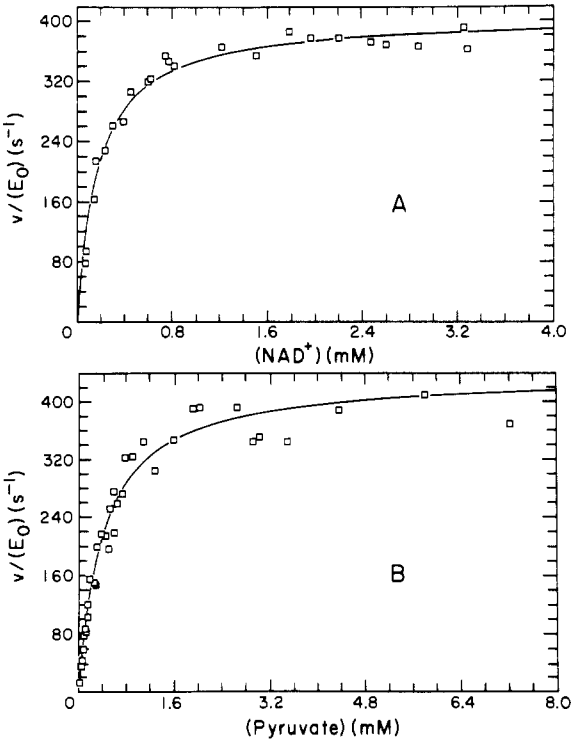

FIGURE 1: (A) A plot of the initial steady-state velocity (v) divided by the molar concentration of the enzyme complex [E_0] vs. the initial concentration of NAD^+ in 0.02 M potassium phosphate (pH 7.0), 4 mM thiamin pyrophosphate, 2 mM $MgSO_4$, 0.2 mM coenzyme A, 0.5 mM dithiothreitol, and 5 mM pyruvate. The curve was calculated by using eq 6 with k_{cat} = 408 s^{-1} and K_m = 0.176 mM. The enzyme concentration was 0.46 nM. (B) A plot of $v/[E_0]$ vs. the initial concentration of pyruvate. The data were obtained under the same conditions as for (A) except the pyruvate concentration was varied, the NAD^+ concentration was fixed at 3 mM, and the enzyme concentration was 0.36 nM. The curve was calculated by using eq 6 with k_{cat} = 426 s^{-1} and K_m = 0.410 mM.

attributed to the binding of NAD^+ at a second site or to inhibition by NADH, a strong inhibitor of the overall reaction. While a distinction between various inhibition mechanisms is not possible, these results indicate that the value of k_{cat} may be somewhat larger than 408–436 s^{-1}.

The time course of the acetylation of the enzyme complex by [3-^{14}C]pyruvate was determined over a range of pyruvate concentrations from 0.02 to 2.1 mM in 0.02 M potassium phosphate (pH 7.0), 4 mM thiamin pyrophosphate, and 2 mM $MgSO_4$ at 4 °C with the quenched stopped-flow technique. The enzyme concentration was 0.16 μM in most cases. In a control experiment, passage of the enzyme complex through the quenched stopped-flow apparatus was shown to have no effect on the catalytic activity. Some typical results are presented in Figure 2 as plots of the logarithm of the fraction of unreacted enzyme complex vs. time. The extent of acetylation at long times (2–5 min) was determined in every kinetic experiment; at long times the number of covalently bound acetyl groups per enzyme molecule of molecular weight 4.8 × 10^6 was 48.4 ± 2.7 (10.1 nmol/mg enzyme complex). As shown in Figure 2, the time course of acetylation is clearly not a simple exponential process. Therefore, in the initial data analysis the data were fit to the equation

$$y = A_1e^{-k_1t} + (1 - A_1)e^{-k_2t} \quad (7)$$

where y is the fraction of unreacted enzyme complex, k_1 and k_2 are rate constants, and A_1 is an amplitude parameter. All of the data were adequately described by eq 7; the rate constants were dependent on the pyruvate concentration, and A_1

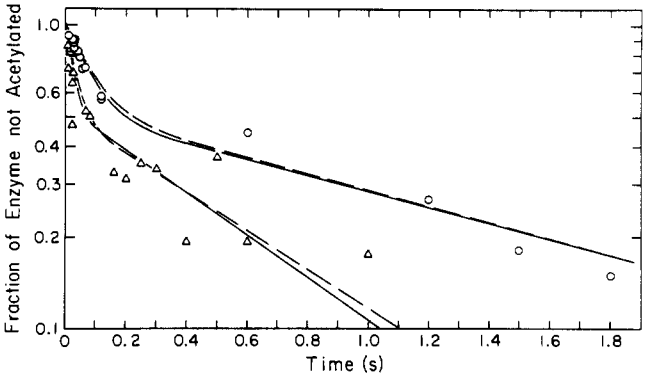

FIGURE 2: Plots of the fraction of enzyme not acetylated by [3-^{14}C]pyruvate vs. time in 0.02 M potassium phosphate (pH 7.0), 4 mM thiamin pyrophosphate, 2 mM $MgSO_4$, 0.16 μM enzyme complex, and (○) 0.13 mM pyruvate or (△) 2.1 mM pyruvate at 4 °C. The curves are the best fits to eq 10 (—) and eq 12 (---).

was ~0.6. The maximum values of the rate constants were approximately 30 s^{-1} (k_1) and 0.6 s^{-1} (k_2). The time course of acetylation at ~1 mM pyruvate was independent of the enzyme concentration over the range 0.069–0.27 μM.

A model for the acetylation mechanism must be assumed to properly analyze the data since complete acetylation requires the 24 E_1 molecules/complex to go through an average of two acetylations before the enzyme is completely acetylated. Three limiting models were considered. All involve the assumptions that each E_1 molecule acetylates two lipoic acids and that the initial binding of pyruvate and enzyme is fast relative to the hydroxyethylation of thiamin pyrophosphate. In model 1, two consecutive acetylation reactions occurring at equal rates were assumed. This can be represented as

$$E_1\text{–}E_2 \xrightarrow{k_1} E_1\text{–}E_2(A)$$

$$E_1\text{–}E_2(A) \xrightarrow{k_1} E_1\text{–}E_2(A,A) \quad (8)$$

where A represents a bound acetyl group and k_1 is dependent on the pyruvate concentration due to the necessary preequilibration between enzyme and pyruvate preceding acetylation which is not shown. For this mechanism

$$y = e^{-k_1t}(1 + 0.5k_1t) \quad (9)$$

The data do not fit eq 9. In model 2, two sets of E_1 molecules were assumed, each set acetylating two lipoic acids with different rate constants k_1 and k_2. If each set of E_1 molecules comprises half of the E_1 molecules/complex, the mechanism can be represented by eq 8 plus an identical pair of equations with rate constant k_2 rather than k_1. For this mechanism

$$y = 0.5e^{-k_1t}(1 + 0.5k_1t) + 0.5e^{-k_2t}(1 + 0.5k_2t) \quad (10)$$

The kinetic data are described well by eq 10 as shown by the two representative least-squares fits of the data in Figure 2. The rate constants obtained are shown as a function of the pyruvate concentration in Figures 3A and 4A. The uncertainty in k_1 is estimated as ±15%, while that in k_2 is ±25%. The rate constant k_2 is less precise than k_1 because more data have been obtained at times when the faster process is of primary importance. The rate constant k_2 is much too small to be of significance in the catalytic process. In model 3, the acetylation was assumed to occur by two *consecutive* reactions with different rate constants.

$$E_1\text{–}E_2 \xrightarrow{k_1} E_1\text{–}E_2(A) \quad (11)$$

$$E_1\text{–}E_2(A) \xrightarrow{k_2} E_1\text{–}E_2(A,A)$$

For this mechanism

$$y = \frac{0.5}{k_2 - k_1}[(2k_2 - k_1)e^{-k_1 t} - k_1 e^{-k_2 t}] \quad (12)$$

The data also are well described by this model as shown by the least-squares fits of the data in Figure 2. The dependence of the rate constants on the pyruvate concentration is shown in Figures 3B and 4B. The comments above concerning the relative errors in the rate constants for model 2 also apply to model 3. The data are equally well fit by models 2 and 3. Other variations of these models would undoubtedly fit the data, but these two classes of mechanisms typify the simplest possibilities.

The dependence of the rate constants on the concentration of pyruvate can be accounted for by assuming pyruvate and the enzyme equilibrate rapidly to form a complex prior to acetylation. This can be represented as

$$E_1\text{–}E_2 + \text{pyruvate} \underset{}{\overset{K}{\rightleftharpoons}} E_1\text{–}E_2\cdot\text{pyruvate} \xrightarrow{k} E_1\text{–}E_2(A) + CO_2 \quad (13)$$

for each of the reactions in eq 8 and 11. Thus

$$k_{1,2} = k/[1 + (K/[\text{pyruvate}])] \quad (14)$$

where $K = [E_1\text{–}E_2][\text{pyruvate}]/[E_1\text{–}E_2\cdot\text{pyruvate}]$. The concentration dependence of k_1 is well described by eq 14 for models 2 and 3. The data in Figures 3A and 4A were fit by a weighted least-squares analysis, and the curves in the figures represent the best fits calculated with eq 14 and $k = 63.7\ s^{-1}$ and $K = 0.477$ mM for model 2 and $k = 40.5\ s^{-1}$ and $K = 0.474$ mM for model 3. The concentration dependence of k_2 also was fit to eq 14, although the scatter in the data is too great to attach anything other than qualitative significance to the parameters derived. The best-fit parameters are $k = 1.74\ s^{-1}$ and $K = 0.119$ mM for model 2 and $k = 1.11\ s^{-1}$ and $K = 0.075$ mM for model 3; the curves in Figures 3B and 4B have been calculated with these parameters and eq 14.

The rate of deacetylation of the enzyme complex with coenzyme A was studied in a series of experiments. If the enzyme complex, preincubated with thiamin pyrophosphate and $MgSO_4$ under the conditions of the acetylation experiments, is mixed with 0.2 mM coenzyme A, 2 mM dithiothreitol, and 0.05 or 1.4 mM pyruvate, the extent of acetylation from 20 ms to 12 s is very small, a few lipoic acids per molecule of enzyme complex. When coenzyme A is not present, acetylation of the enzyme is not altered by the presence of dithiothreitol in the concentration range 1.6–4.4 mM. These results indicate the rate constant for deacetylation is much larger than the rate constant for acetylation.

If the enzyme is incubated with 4 mM thiamin pyrophosphate, 2 mM $MgSO_4$, and 0.64 mM [3-^{14}C]pyruvate in 0.02 M potassium phosphate (pH 7) at 0 °C for times longer than ~1 min, coenzyme A cannot completely deacetylate the enzyme complex: some fraction of the acetyl groups appears to be irreversibly bound to the enzyme complex. In Figure 5 the number of irreversibly bound acetyl groups per molecule of enzyme complex is shown as a function of the incubation time before deacetylation with coenzyme A for 10 min. After 10 min, the protein was precipitated with perchloric acid for analysis in the usual manner. No significant difference in the results was observed when deacetylation was carried out with 0.2 mM coenzyme A and 2 mM dithiothreitol, 0.3 mM coenzyme A and 2 mM dithiothreitol plus 6 mM NAD^+, or 0.3 mM coenzyme A and 2 mM dithiothreitol plus 6 mM NAD^+, 4 mM thiamin pyrophosphate, 2 mM $MgSO_4$, and 7 mM unlabeled pyruvate. At sufficiently long incubation times, all of the labeled acetyl groups become irreversibly bound to the enzyme. However, as shown in Figure 5, the enzyme complex retains 70% or more of its catalytic activity throughout the time span of these experiments. If the enzyme is acetylated with unlabeled pyruvate by incubation for 100 min under the

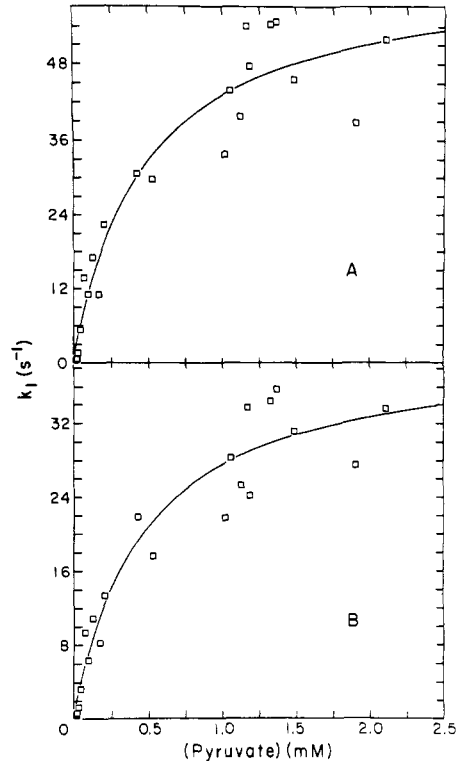

FIGURE 3: Plots of the rate constant k_1 vs. the concentration of pyruvate, where k_1 is defined by eq 10 (A) or eq 12 (B). The line in (A) was calculated by using eq 14 with $k = 64.7\ s^{-1}$ and $K = 0.477$ mM; the line in (B) was calculated by using eq 14 with $k = 40.5\ s^{-1}$ and $K = 0.474$ mM. The data were obtained in 0.02 M potassium phosphate (pH 7.0), 4 mM thiamin pyrophosphate, and 2 mM $MgSO_4$ at 4 °C with 0.069–0.27 μM enzyme.

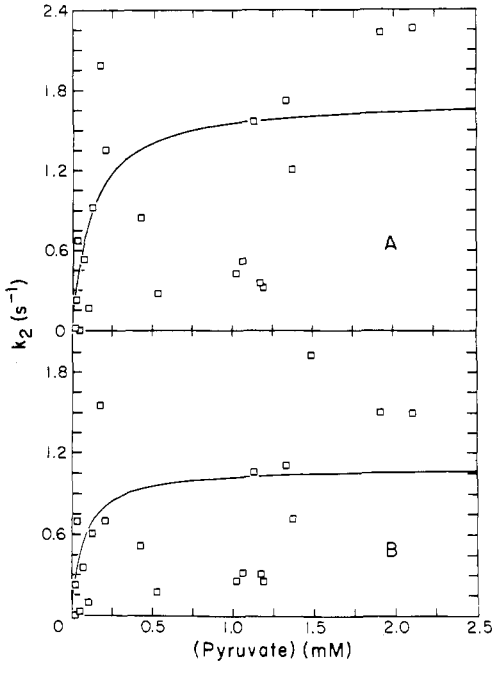

FIGURE 4: Plots of the rate constant k_2 vs. the pyruvate concentration where k_2 is defined by eq 10 (A) or eq 12 (B). The line in (A) was calculated by using eq 14 with $k = 1.74\ s^{-1}$ and $K = 0.119$ mM; the line in (B) was calculated by using eq 14 with $k = 1.11\ s^{-1}$ and $K = 0.075$ mM. The experimental conditions were the same as in Figure 3.

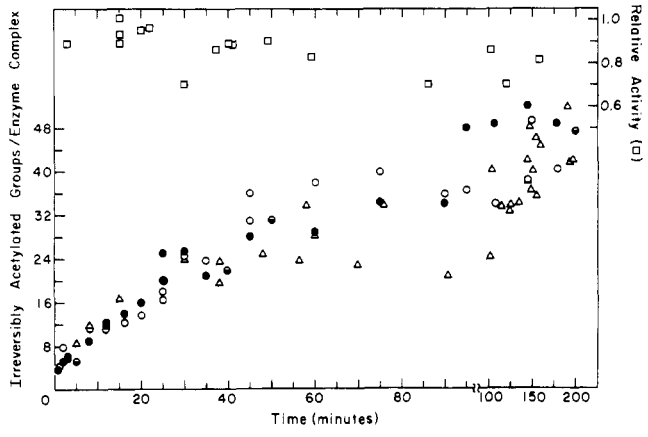

FIGURE 5: A plot of the number of irreversibly acetylated groups per enzyme complex vs. the incubation time of the enzyme complex in 0.64 mM pyruvate, 0.02 M potassium phosphate (pH 7.0), 4 mM thiamin pyrophosphate, and 2 mM $MgSO_4$ at 0 °C. Deacetylation of the enzyme complex was carried out for 10 min under the same conditions in the presence of the following: (●) 0.2 mM coenzyme A and 2 mM dithiothreitol; (○) 0.3 mM coenzyme A, 2 mM dithiothreitol, and 6 mM NAD^+; or (△) 0.3 mM coenzyme A, 2 mM dithiothreitol, 6 mM NAD^+, 4 mM thiamin pyrophosphate, 2 mM $MgSO_4$, and 7 mM pyruvate. In each case the enzyme concentration was 0.24 μM. The relative activity of the enzyme also is shown (□).

conditions used to obtain the data in Figure 4, addition of 0.64 mM [3-^{14}C]pyruvate, 4 mM thiamin pyrophosphate, and 2 mM $MgSO_4$, followed by an additional 10-min incubation, resulted in the incorporation of up to 48 labeled acetyl groups into the enzyme complex. In similar experiments, when the labeled pyruvate was used in the initial incubation mixture, more than 90 acetyl groups per molecule of enzyme complex were found. These results indicate that the acetyl groups originally on lipoic acids are slowly transferred to other functional groups on the protein that are not essential for catalytic activity.

Discussion

The steady-state kinetic data in Figure 1 indicate that simple Michaelis–Menten kinetics are found with both NAD^+ and pyruvate at 4 °C. A sigmoidal kinetic isotherm for pyruvate at very low pyruvate concentrations has been reported at 30 and 37 °C with enzyme from K-12 *E. coli* (Bisswanger & Henning, 1971); however, no significant deviations from a hyperbolic isotherm were observed in our experiments. The observed value of the Michaelis constant, 0.410 mM, is in reasonable agreement with that found for the pyruvate dehydrogenase complex from Crooke's *E. coli* [0.51 mM, Schwartz et al. (1968)] and *Azotobacter vinelandii* [0.3 mM, Bresters et al. (1975)].

The labeling of the lipoic acids in the presence of thiamin pyrophosphate and pyruvate with maleimides (Grande et al., 1975; Danson & Perham, 1976; Shepherd & Hammes, 1977) and with labeled pyruvate (Speckhard et al., 1977; Bates et al., 1977) has been well documented. The average value of 48 covalently bound acetyl groups per enzyme complex found at long times is in agreement with earlier results (Collins & Reed, 1977; Bates et al., 1977; Frey et al., 1978) and suggests two lipoic acids per polypeptide chain of E_2 are present [cf. Collins & Reed (1977)].

The time course of acetylation indicates two distinct rate processes, with about half of the acetylation occurring through each process. The kinetic data do not distinguish between each E_1 being associated with fast *or* slow acetylation reactions (model 2) or fast *and* slow acetylation reactions (model 3). More complex models where all E_1 molecules do not participate in the same number of acetylation reactions have not been tested. For both models tested, the equilibrium dissociation constant for the binding of pyruvate to the enzyme (K) obtained from the concentration dependence of k_1 is similar to the Michaelis constant obtained from the steady-state data and the equilibrium constant obtained from direct binding measurements [0.31 mM, Shepherd & Hammes (1976)]. In terms of the mechanism depicted in eq 1–3, the dependence of k_1 on the pyruvate concentration requires the rate-determining step to be the first irreversible step which probably is the formation of the (hydroxyethyl)thiamin pyrophosphate.

The rate of acetylation of the K-12 *E. coli* complex at a single pyruvate concentration (0.036 mM) has been reported (Danson et al., 1978). The rate is similar to that found in this work, but the multiple kinetic processes are difficult to resolve at this pyruvate concentration. Moreover, we have found the quenching and washing procedure used with trichloroacetic acid to result in a significant loss of label from the protein. The time course of acetylation of the mammalian pyruvate dehydrogenase complex also has been reported to be biphasic (Davis et al., 1979).

The deacetylation of the enzyme by coenzyme A is much more rapid than the acetylation. The slow transfer of acetyl groups from lipoic acid to dead-end products in the absence of coenzyme A is consistent with earlier experiments (Frey et al., 1978). The location of the dead-end sites is unknown, but the catalytic activity is not significantly influenced by their labeling. This process is unlikely to be of physiological importance.

The limiting values of k_1 at high pyruvate concentrations (63.7 and 40.5 s^{-1} for models 2 and 3, respectively) can be compared with the turnover number per mole of enzyme complex, 420 s^{-1}, by assuming a value for the number of sites on the complex participating in the rate-determining step. In the steady state a *single* acetylation is associated with each turnover. Since deacetylation of lipoic acids by coenzyme A and reoxidation of lipoic acids do not appear to be rate limiting (this work; Angelides & Hammes, 1978), the rate-determining step most likely occurs on E_1. If all 24 E_1 subunits participate in the catalytic cycle, the turnover number per catalytic site is 17.5 s^{-1}. This is significantly less than the limiting rate constants for acetylation. The simplest explanation for the discrepancy between the acetylation rate constants and the turnover number is that only a fraction of the E_1 molecules participate in catalysis. For example, if only 12 E_1 molecules participate, the turnover number per E_1 molecule is 35 s^{-1}. Other results have suggested that not all of the acetylation reactions are coupled into the normal catalytic process (Frey et al., 1978; Angelides & Hammes, 1978). However, alternative explanations are that the turnover number may be underestimated because of the inhibition occurring at high concentrations of NAD^+, or the rates of the initial acetylation of the complex may be slower than those of acetylation in the steady state. The results obtained cannot distinguish between these mechanistic possibilities.

Acknowledgments

The authors thank Professor George Hess and Dr. Derek Cash for the use of their quenched-flow apparatus in preliminary experiments and for their help and advice.

References

Akiyama, S. K. (1980) Ph.D. Thesis, Cornell University, Ithaca, NY.

Angelides, K. J., & Hammes, G. G. (1978) *Proc. Natl. Acad. Sci. U.S.A. 75*, 4877–4880.

Angelides, K. J., & Hammes, G. G. (1979) *Biochemistry 18*, 1223–1229.
Angelides, K. J., Akiyama, S. K., & Hammes, G. G. (1979) *Proc. Natl. Acad. Sci. U.S.A. 76*, 3279–3283.
Bates, D. L., Danson, M. J., Hale, G., Hooper, E. A., & Perham, R. N. (1977) *Nature (London) 268*, 313–316.
Bisswanger, H., & Henning, U. (1971) *Eur. J. Biochem. 24*, 376–384.
Bresters, T. W., De Abreu, R. A., De Kok, A., Visser, J., & Veeger, C. (1975) *Eur. J. Biochem. 59*, 335–345.
Brown, J. P., & Perham, R. N. (1976) *Biochem. J. 155*, 419–427.
Collins, J. H., & Reed, L. J. (1977) *Proc. Natl. Acad. Sci. U.S.A. 74*, 4223–4227.
Danson, M. J., & Perham, R. N. (1976) *Biochem. J. 159*, 677–682.
Danson, M. J., Fersht, A. R., & Perham, R. N. (1978) *Proc. Natl. Acad. Sci. U.S.A. 75*, 5386–5390.
Davis, L. C., Cate, R. L., & Roche, T. E. (1979) *Anal. Biochem. 97*, 428–437.
Fersht, A. R., & Jakes, R. (1975) *Biochemistry 14*, 3350–3356.
Frey, P. A., Ikeda, B. H., Gavino, G. R., Speckhard, D. C., & Wong, S. S. (1978) *J. Biol. Chem. 253*, 7234–7241.
Grande, H. J., Bresters, T. W., De Abreu, R. A., De Kok, A., & Veeger, C. (1975) *Eur. J. Biochem. 59*, 355–363.
Koike, M., Reed, L. J., & Carroll, W. R. (1960) *J. Biol. Chem. 235*, 1931–1938.
Koike, M., Reed, L. J., & Carroll, W. R. (1963) *J. Biol. Chem. 238*, 30–39.
Lowry, O. H., Rosebrough, N. J., Farr, A. L., & Randall, R. J. (1951) *J. Biol. Chem. 193*, 265–275.
Lymn, R. W., & Taylor, E. W. (1970) *Biochemistry 9*, 2975–2983.
Meister, A. (1950) *J. Biol. Chem. 184*, 117–129.
Moe, O. A., Lerner, D. A., & Hammes, G. G. (1974) *Biochemistry 13*, 2552–2557.
Neish, W. (1957) *Methods Biochem. Anal. 5*, 107–179.
Reed, L. J. (1974) *Acc. Chem. Res. 7*, 40–46.
Reed, L. J., & Willms, C. R. (1966) *Methods Enzymol. 9*, 246–265.
Schwartz, E. R., Old, L. O., & Reed, L. J. (1968) *Biochem. Biophys. Res. Commun. 31*, 495–500.
Shepherd, G. B., & Hammes, G. G. (1976) *Biochemistry 15*, 311–317.
Shepherd, G. B., & Hammes, G. G. (1977) *Biochemistry 16*, 5234–5240.
Speckhard, D. C., Ikeda, B. H., Wong, S. S., & Frey, P. A. (1977) *Biochem. Biophys. Res. Commun. 77*, 708–713.
Willms, C. R., Oliver, R. M., Henney, H. R., Mukherjee, B. B., & Reed, L. J. (1967) *J. Biol. Chem. 242*, 889–897.

Relationship of Transmembrane pH and Electrical Gradients with Respiration and Adenosine 5′-Triphosphate Synthesis in Mitochondria†

Andrij Holian* and David F. Wilson

ABSTRACT: The mechanism of mitochondrial oxidative phosphorylation and its regulation have been studied by using suspensions of isolated rat liver mitochondria. Parallel measurements were made of mitochondrial volume, respiration, transmembrane pH and electrical gradients, and adenosine 5′-triphosphate (ATP), adenosine 5′-diphosphate (ADP), and inorganic phosphate (P_i) concentrations under various experimental conditions. The transmembrane electrical gradients were calculated from the equilibrium distributions of [^{3}H]-triphenylmethylphosphonium ($TPMP^+$), [^{3}H]tribenzylmethylammonium ($TBMA^+$), and K^+ (plus valinomycin). The transmembrane distributions of labeled acetate, methylamine, and 5,5-dimethyloxazolidine-2,4-dione were used for the calculation of pH gradients. Evaluation of the data shows that the respiratory rate is strictly correlated with [ATP]/([ADP][P_i]) (free energy of ATP synthesis), whereas there is no consistent correlation between the transmembrane electrical potential, the pH gradient, or the total "protonmotive force" ($\Delta\mu_{H^+}$) and the respiratory rate. Thermodynamic analysis indicates that, in order for the proton electrochemical gradient to serve as an intermediate in ATP synthesis, from three to seven H^+ would have to be transported per each ATP synthesized, depending on the experimental conditions. These results suggest that the proton electrochemical gradient may not serve as a primary intermediate in oxidative phosphorylation.

The obligatory parameters of any intermediate(s) (I) between the oxidation–reduction reactions and ATP synthesis in mitochondrial oxidative phosphorylation can be determined from accurate kinetic and thermodynamic (free energy) measurements. Experimental evidence has been obtained that the first two sites of oxidative phosphorylation are in near equilibrium (Erecinska et al., 1974; Wilson et al., 1974a,b), and the overall rate of oxidative phosphorylation is regulated by extramitochondrial (Holian et al., 1977; Owen & Wilson, 1974; Wilson et al., 1977) or cytosolic (Wilson et al., 1974a,b; Erecinska et al., 1977) [ATP]/([ADP][P_i]). Therefore, intermediates in oxidative phosphorylation must fit the required relationship for the free energy change in the oxidation–reduction reactions to that utilized in ATP synthesis

$$\Delta G_{O\text{-}R} \geq \Delta G_I \geq \Delta G_{ATP} \quad (1)$$

where $\Delta G_{O\text{-}R}$, ΔG_I, and ΔG_{ATP} are the free energy changes associated with the oxidation–reduction reactions, the inter-

† From the Department of Biochemistry and Biophysics, University of Pennsylvania, Medial School, Philadelphia, Pennsylvania 19104. *Received December 6, 1979.* This work was supported by National Institutes of Health Grants GM21524 and GM12202.

0006-2960/80/0419-4213$01.00/0